Supporting Information (SI)

Nitrogen-free *TM*S_4-centers in metal–organic frameworks for ammonia synthesis

Xingshuai Lv,[a] Wei Wei,[*,a] Hao Wang,[a] Fengping Li,[a] Baibiao Huang,[a] Ying Dai[*,a] and Timo Jacob[*,b]

[a] *School of Physics, State Key Laboratory of Crystal Materials, Shandong University, 250100 Jinan, China*

[b] *Institute of Electrochemistry, Ulm University, Albert-Einstein-Allee 47, D-89081 Ulm, Germany*

[*]Corresponding authors:

weiw@sdu.edu.cn (W. Wei)

daiy60@sdu.edu.cn (Y. Dai)

timo.jacob@uni-ulm.de (T. Jacob)

1. Stabilities of Sc– and Mo–BHT

Stabilities of proposed Sc– and Mo–BHT for NRR were confirmed. Cohesive energies (E_{coh}) for Sc– and Mo–BHT are 5.62 and 5.47 eV/atom, larger than those of the already-synthesized Cu–BHT (5.11 eV/atom) and Ni–BHT (5.41 eV/atom), confirming stability of these alternative MOFs. It is also indicative that Sc–BHT and Mo–BHT can be with significantly large possibility synthesized under certain experimental conditions.[1,2] In Figures S2a and b, the phonon dispersion spectra of Sc–

and Mo–BHT show that the low-frequency optical and acoustic branches are well-separated from each other at the Γ point and no imaginary phonon frequencies can be observed over the entire Brillouin zone, indicative of the perfect dynamic stability. In addition, AIMD simulations at 500 K were further performed for Sc– and Mo–BHT. As shown in Figures S2c and d, the total energies oscillate within a small range and snapshots of structures after 10 ps indicate no obvious structural deformation, confirming thermal stability at even elevated temperature.

2. Microkinetic modeling

The following elementary reaction steps constituting the ammonia synthesis are considered

$$N_2\,(g) + * \leftrightarrow N_2* \quad \text{(R1)}$$

$$H_2\,(g) + 2* \leftrightarrow 2H* \quad \text{(R2)}$$

$$N_2* + H* \leftrightarrow N_2H* + * \quad \text{(R3)}$$

$$N_2H* + H* \leftrightarrow N_2H_2* + * \quad \text{(R4)}$$

$$N_2H_2* + H* \leftrightarrow N* + *\ (NH_3\ \text{release}) \quad \text{(R5)}$$

$$N* + H* \leftrightarrow NH* + * \quad \text{(R6)}$$

$$NH* + H* \leftrightarrow NH_2* + * \quad \text{(R7)}$$

$$NH_2* + H* \leftrightarrow NH_3* + * \quad \text{(R8)}$$

$$NH_3* \leftrightarrow NH_3\,(g) + * \quad \text{(R9)}$$

where * denotes a free active site (a metal atom). The rate of each elementary step can be written as

$$r_1 = k_1 p_{N_2} \theta_* - k_{-1} \theta_{N_2^*} \quad (1)$$

$$r_2 = k_2 p_{H_2} \theta_*^2 - k_{-2} \theta_{H^*}^2 \quad (2)$$

$$r_3 = k_3 \theta_{N_2^*} \theta_{H^*} - k_{-3} \theta_{N_2H^*} \theta_* \quad (3)$$

$$r_4 = k_4 \theta_{N_2H^*} \theta_{H^*} - k_{-4} \theta_{N_2H_2{}^*} \theta_* \quad (4)$$

$$r_5 = k_5 \theta_{N_2H_2{}^*} \theta_{H^*} - k_{-5} \theta_{N^*} \theta_* \quad (5)$$

$$r_6 = k_6 \theta_{N^*} \theta_{H^*} - k_{-6} \theta_{NH^*} \theta_* \quad (6)$$

$$r_7 = k_7 \theta_{NH^*} \theta_{H^*} - k_{-7} \theta_{NH_2{}^*} \theta_* \quad (7)$$

$$r_8 = k_8 \theta_{NH_2{}^*} \theta_{H^*} - k_{-8} \theta_{NH_3{}^*} \theta_* \quad (8)$$

$$r_9 = k_9 \theta_{NH_3{}^*} - k_{-9} p_{NH_3} \theta_* \quad (9)$$

where k represents the rate constant of a reaction process, p denotes the partial pressure of gas N_2, H_2 and NH_3, θ denotes the coverage of the adsorbed species.

For Mo–BHT, the elementary step R6 is the rate-determining step (RDS), which is much slower than the other steps because of the much higher kinetic barrier. Therefore, the coverage of reaction species can be solved analytically under the quasi-equilibrium approximation (QEA),[3,4] where the reaction rates of the fast step j (j = R1, R2, R3, R4,

R5, R7, R8 and R9) in the forward and backward direction are the same (r=0), that is r_j = r_{-j}. Hence, the following equations can be obtained

$$\theta_{N_2^*} = K_1 p_{N_2} \theta_* \tag{10}$$

$$\theta_{H^*} = \sqrt{K_2 p_{H_2}}\,\theta_* \tag{11}$$

$$\theta_{N_2H^*} = \frac{K_3 \theta_{N_2^*} \theta_{H^*}}{\theta_*} \tag{12}$$

$$\theta_{N_2H_2{}^*} = \frac{K_3 K_4 \theta_{N_2^*} \theta_{H^*}^2}{\theta_*^2} \tag{13}$$

$$\theta_{N^*} = \frac{K_3 K_4 K_5 \theta_{N_2^*} \theta_{H^*}^3}{\theta_*^3} \tag{14}$$

$$\theta_{NH^*} = \frac{p_{NH_3} \theta_*^3}{K_7 K_8 K_9 \theta_{H^*}^2} \tag{15}$$

$$\theta_{NH_2{}^*} = \frac{p_{NH_3} \theta_*^2}{K_8 K_9 \theta_{H^*}} \tag{16}$$

$$\theta_{NH_3{}^*} = \frac{p_{NH_3} \theta_*}{K_9} \tag{17}$$

where $K_i = k_i/k_{-i}$ is the equilibrium constant for step i, which can be expressed by

$$K_i = e^{\frac{-\Delta G_i}{k_B T}} \tag{18}$$

$$k_i = v_1 e^{\frac{-\Delta G_a}{k_B T}} \approx \frac{k_B T}{h} e^{\frac{-\Delta G_a}{k_B T}} \tag{19}$$

where ΔG_i and ΔG_a are free energies of reaction/activation respectively. The sum of coverage of all the reaction species θ_i is set to 1 for each site

$$\sum_i \theta_i = 1 \tag{20}$$

The conversion ratio of NH_3 was fixed as 10%.[5] Combining equation (10-20), θ* can be solved analytically. Then, the coverage of various reaction species and the rate of R6 can be obtained.

Table S1 Spin moment on TM atom (μ), number of valence electrons in *d* orbital of TM atom (φ_d), number of valence electrons of TM atom ($\varphi_{valence}$), electronegativity of TM atom (ζ) and oxidation state of TM atom (λ). ψ is defined as $\psi = \varphi_d \times (\zeta_{TM} + 4\zeta_S)$.

Atom	μ	φ_d	$\varphi_{valence}$	ζ	$\varphi_d \times \zeta$	$\varphi_{valence} \times \zeta$	ψ	λ

Sc	0.21	1	3	1.36	1.36	4.08	11.68	1.60
Ti	1.83	2	4	1.54	3.08	6.16	23.72	1.24
V	2.84	3	5	1.63	4.89	8.15	35.85	1.10
Fe	1.92	6	8	1.83	10.98	14.64	72.90	0.73
Co	0.70	7	9	1.88	13.16	16.92	85.40	0.55
Mo	1.74	5	6	2.16	10.8	12.96	62.40	0.90

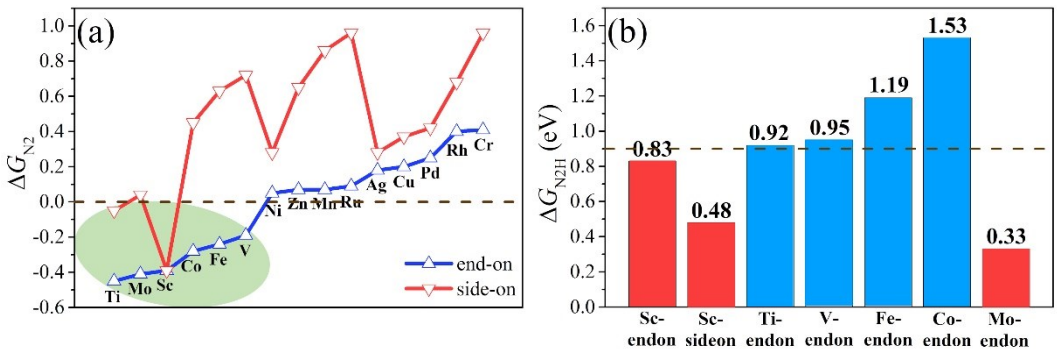

Figure S1 Gibbs free energy change of (a) $^*N_2$ and (b) $^*N_2H$ species on *TM*–BHTs.

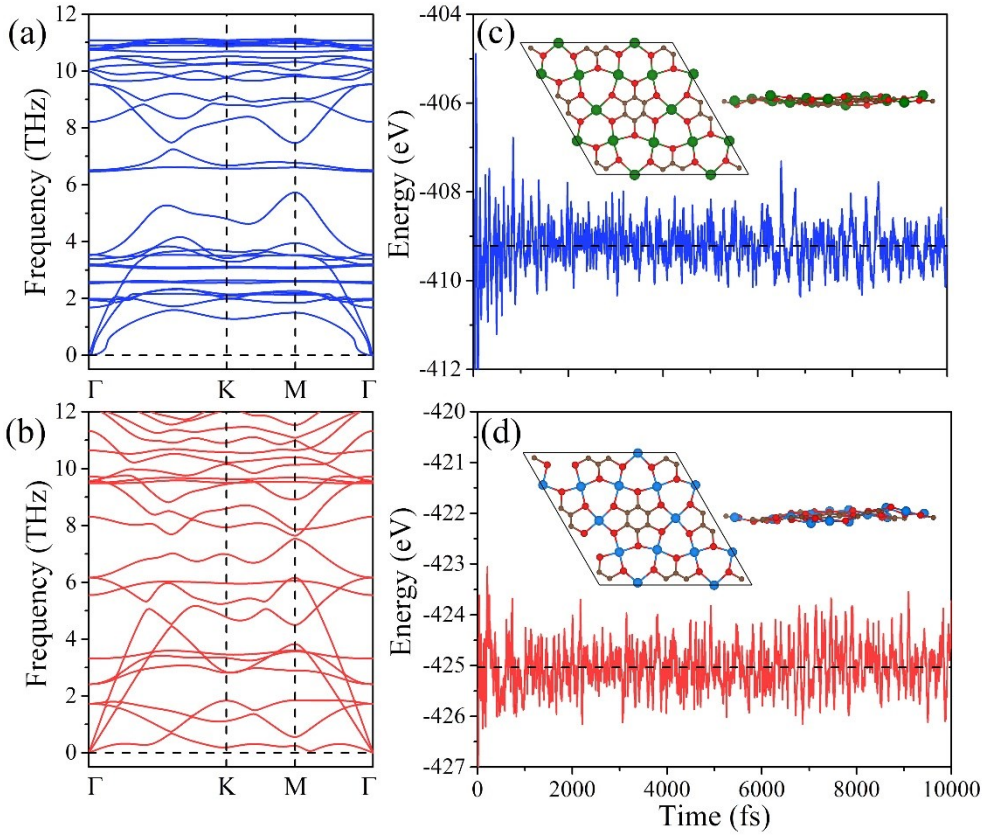

Figure S2 Phonon dispersion spectra of (a) Sc– and (b) Mo–BHT. Total energy as a function of time at 500 K during AIMD simulations for (c) Sc– and (d) Mo–BHT. Insets are structures after 10 ps AIMD simulations.

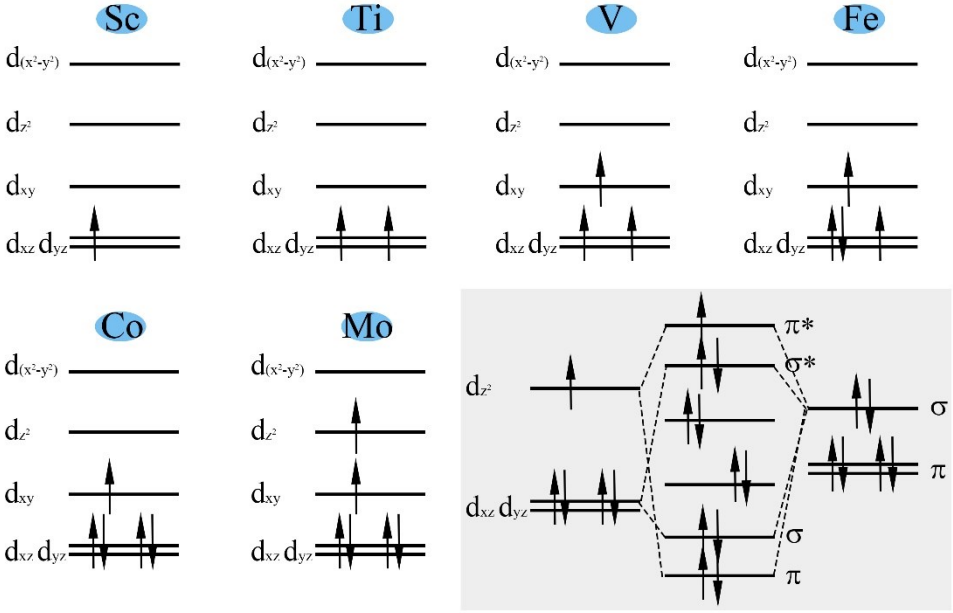

Figure S3 Electronic configurations of various TM atoms. The orbital interactions between Mo sites and the N_2 molecule is also shown.

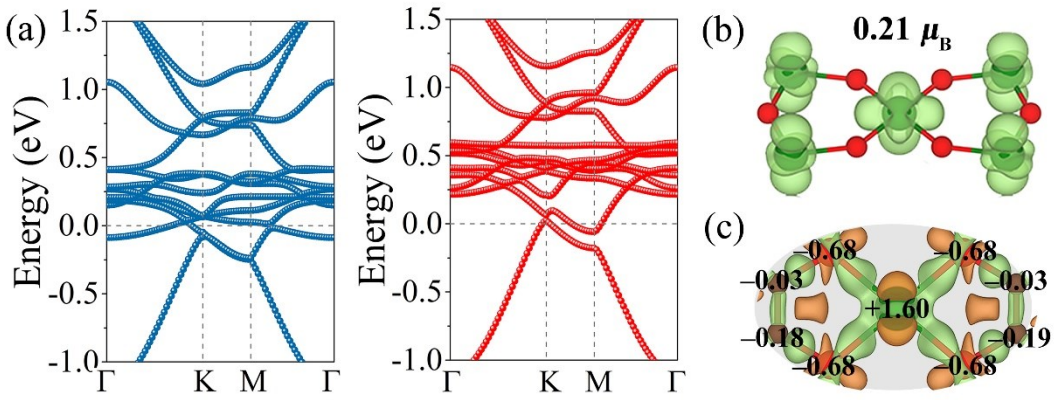

Figure S4 Electronic property of Sc–BHT, including (a) band structure, (b) spin-resolved density (SRD) and (c) charge density difference (CDD) with Bader charge denoted.

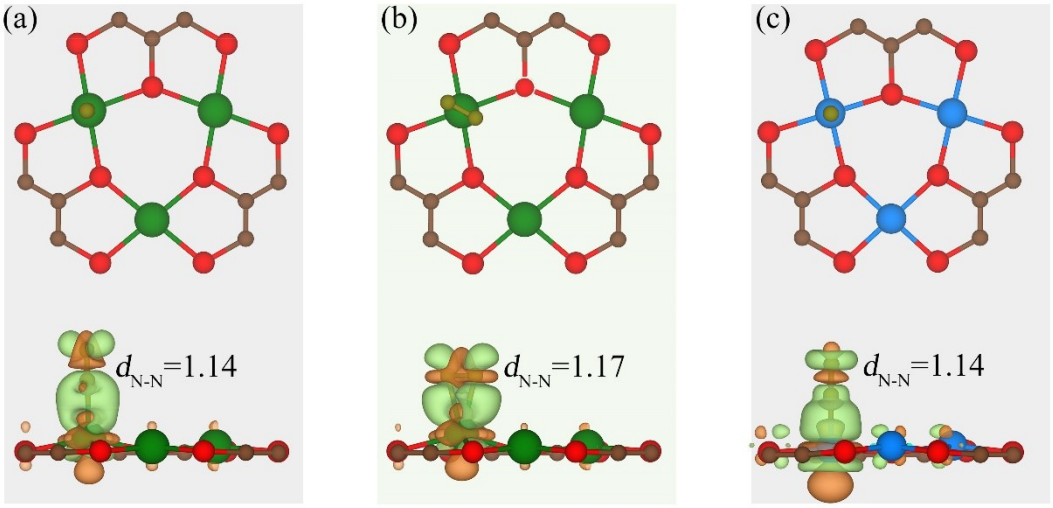

Figure S5 Optimized structures and charge density difference of N_2 adsorption on Sc–BHT via (a) end-on and (b) side-on patterns and (c) on Mo–BHT via end-on pattern. The isovalue is set to 0.002 e/Å^3. The bond lengths of N–N are also given.

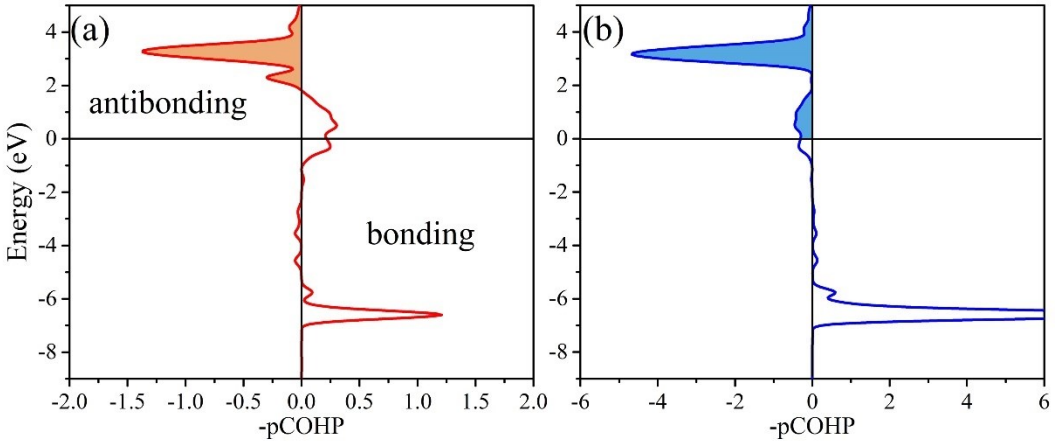

Figure S6 -pCOHP of (a) TM–N bond and (b) N–N bond, where the shaded areas represent the antibonding states higher than E_F. It can be seen that the energy of the N≡N antibonding states locate in the range from 0 to 4.0 eV, which is closer to the E_F compared with that of Mo–N bond (from 1.5 to 4.0 eV).

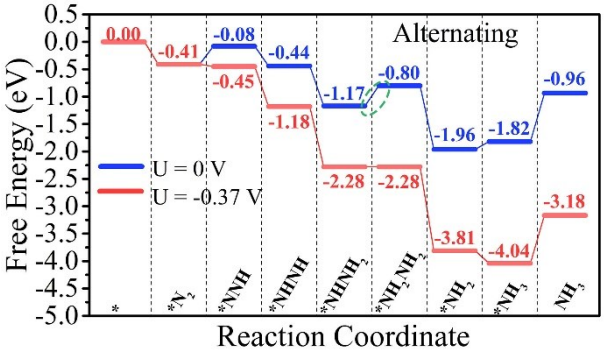

Figure S7 Free energy diagram at each hydrogenation step on Mo–BHT via alternative pathway of NRR. The potential-limiting step is highlighted with green circle.

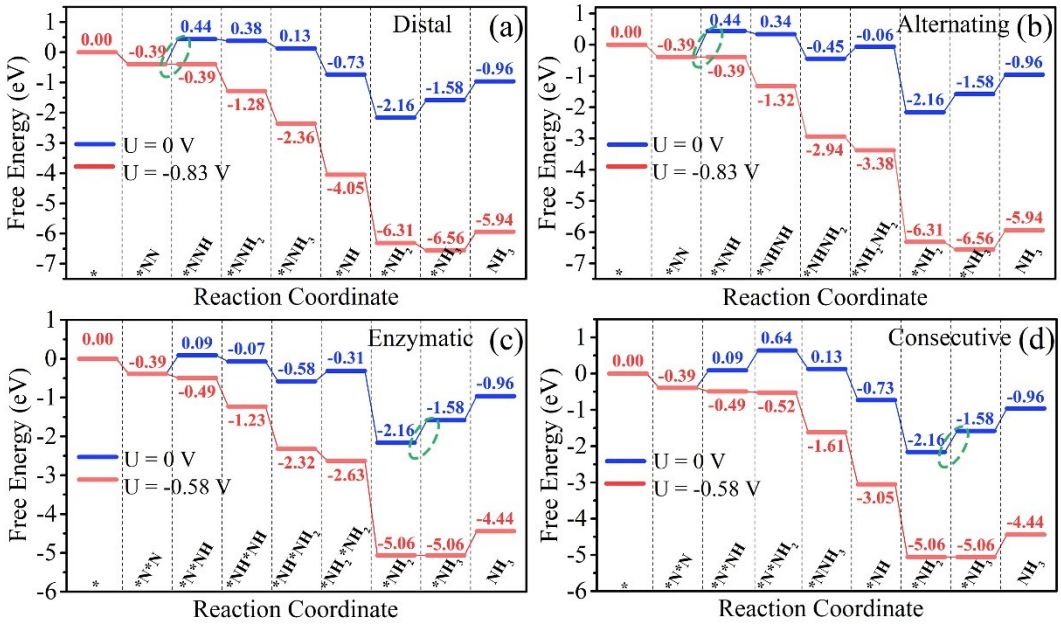

Figure S8 Free energy diagrams for NRR on Sc–BHT through (a) distal, (b) alternating, (c) enzymatic and (d) consecutive pathways. The potential-limiting steps are highlighted with green circles.

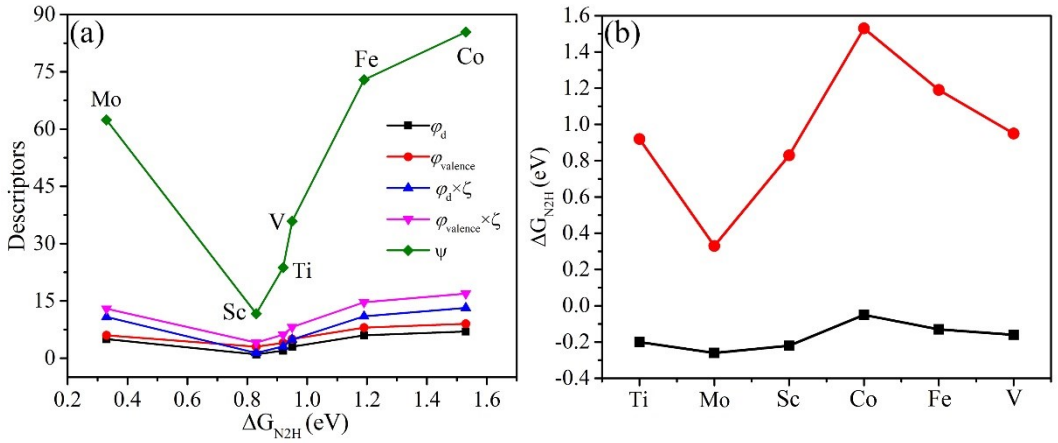

Figure S9 (a) Relationship between the five descriptors with ΔG_{N_2H}. Good linear relationship (R^2 = ~0.90) exists between each descriptor and G_{N_2H} for Sc, Ti, V, Fe and Co–BHT. (b) ΔG_{N_2H} and dipole moments of the adsorbed N_2 molecule.

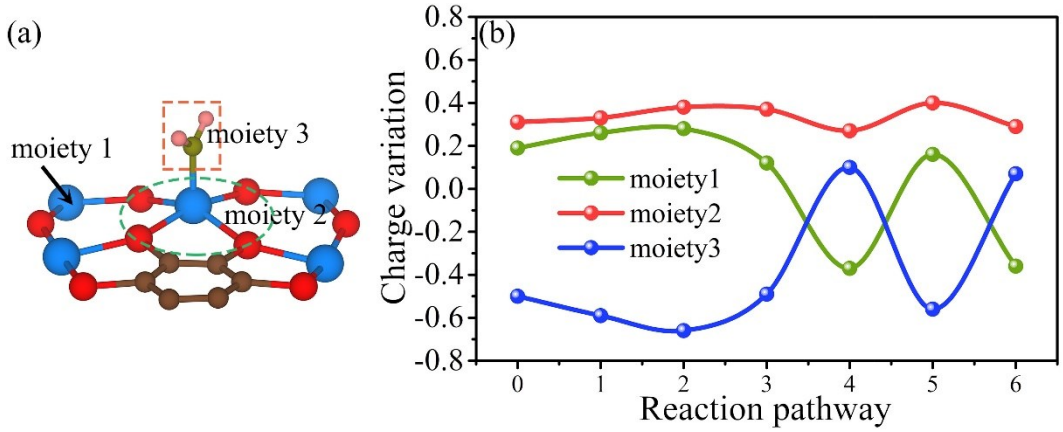

Figure S10 (a) For example, three moieties of the *TM*–BHT═NH_2 intermediate, and (b) charge variation of the three moieties along the enzymatic pathway of Sc–BHT.

References

1 T. Yu, Z. Zhao, L. Liu, S. Zhang, H. Xu and G. Yang, *J. Am. Chem. Soc.*, 2018,

140, 5962−5968.

2 T. Yu, Z. Zhao, Y. Sun, A. Bergara, J. Lin, S. Zhang, H. Xu, L. Zhang, G. Yang and Y. Liu, *J. Am. Chem. Soc.*, 2019, **140**, 1599−1605.

3 H. Lynggaard, A. Andreasen, C. Stegelmann and P. Stoltze, *Prog. Surf. Sci.*, 2004, **77**, 71−137.

4 P. Stoltze, *Prog. Surf. Sci.*, 2000, **65**, 65−150.

5 J.-C. Liu, X.-L. Ma, Y. Li, Y. G. Wang, H. Xiao and J. Li, *Nat. Commun.*, 2018, **9**, 1610.